TÜBİTAK

Turkish Journal of Chemistry

http://journals.tubitak.gov.tr/chem/

Research Article

Turk J Chem
(2016) 40: 305 – 313

doi:10.3906/kim-1502-67

Enhanced delivery of epirubicin by polyoxometalate-based magnetic nanocarriers: controlled drug loading and pH-sensitive drug release

Ezzat RAFIEE*, Nasibeh RAHPEYMA
Faculty of Chemistry, Razi University, Kermanshah, Iran

Received: 11.02.2015 • **Accepted/Published Online:** 22.09.2015 • **Final Version:** 02.03.2016

Abstract: A series of polyoxometalate-based magnetic nanoparticles were developed as novel carriers for anticancer drugs. Characterization of the nanoparticles was done by transmission electron microscopy (TEM), scanning electron microscopy (SEM), Fourier transform infrared spectroscopy (FTIR), wavelength dispersive X-ray (WDX), and laser particle size analyzer. Epirubicin (EPI) was selected as a model drug. EPI loading efficiency, EPI loading content, and EPI release profiles were studied. Drug loading was controlled using acid-base titration since H^+ was released during the loading process. Based on these investigations, an efficient EPI delivery system was introduced. It showed high EPI-loading capacity (35.2 wt.%) and high EPI loading efficiency (97.9%). The EPI release in acetate buffer (87.7%) was greater than that in phosphate buffered saline (51.2%). The pH-sensitive release, high EPI loading content, and excellent EPI loading efficiency are the main benefits of the presented drug delivery system. The pH-sensitive release of EPI may decrease its cytotoxicity. Moreover, the magnetic carrier could be used as a contrast agent in magnetic resonance imaging.

Key words: Epirubicin, magnetic nanocarrier, controlled drug loading, pH-sensitive release, cobalt ferrite, polyoxometalate

1. Introduction

In recent years, controlled drug delivery using nanostructured functional materials has been attracting increasing attention.[1,2] Magnetic nanocarriers (MNCs) are useful for various applications, such as drug delivery and magnetic resonance imaging (MRI). Recently, much attention has been focused on the use of MNCs in the field of cancer studies.[3–6] Nanovectors based on the three magnetic elements Co, Ni, and Fe were used as MNCs to minimize the cytotoxicity of anticancer drugs through mediating a hyperthermic effect and/or transportation of drugs to cancer tissues.[6–8] To date, many MNCs have been used for anticancer drugs, including anthracyclines.[9–20]

Doxorubicin hydrochloride and epirubicin hydrochloride (EPI) are the main anthracycline drugs in the treatment of breast cancer.[21,22] EPI is a 4'-epimer of doxorubicin and shows less toxicity compared with the widely popular doxorubicin. However, most of the studies on anthracycline-loaded MNCs were performed with doxorubicin.[9–19] Few investigations with EPI have been reported.[20] Using EPI in cancer chemotherapy eliminates a number of side effects.[23,24] However, several problems have restricted the clinical and in vivo applications of EPI-loaded MNCs.[25] Therefore, the development of new multifunctional MNCs brings new hope to the field of cancer research.

*Correspondence: ezzat_rafiee@yahoo.com

In the design of MNCs, one of the critical requirements is the nonbiodegradability or intact excretion of the magnetic core. Therefore, to avoid exposure of the core, it has to be coated to facilitate use of MNCs in an acid or alkaline environment. Various kinds of stabilization materials including SiO_2, carbon, and polymeric matrix have been used for this purpose.[6] The unique characteristics of silica materials, including good biocompatibility, chemically modi?able surface, chemical stability, good mechanical strength, and thermal resistance, have made them excellent candidates for coating, enzyme immobilization, and drug delivery.[1,2] For pure silica, only weak intermolecular hydrogen bonds are formed between surface Si–OH group and drugs. Such interactions are suitable for efficient drug loading and drug release.

Surface functionalization could be used for regulation of drug loading and drug release mechanism of MNCs through changing their hydrophobicity/hydrophilicity and electrostatic interactions with drugs. A number of studies were focused on the use of organic modified silica as drug carrier.[26] These studies showed limited chemical and mechanical stability, swelling, and susceptibility to microbiological attack. Because of these facts, inorganic molecules are a promising choice and are a topic of intense research.[6]

In this work, we designed and synthesized a series of novel MNCs for targeted EPI-delivery. Silica encapsulated cobalt ferrite (CoFe@Si) nanoparticles were used as magnetic cores. Polyoxometalates (POMs) were chosen for their inorganic function for modification of the silica surface. These early transition metal oxygen anion clusters continue to find application in medicine. It is known that POMs have a broad spectrum of antiviral and anticancer activities.[27–31] In addition, the existence of numerous oxygen and hydrogen atoms in POM structures makes the MNCs stable in polar media and provide suitable sites for drug/carrier interactions.

The present study focused on the physicochemical aspects of the preparation and characterization of POM-based MNCs for morphology, size distribution, and EPI loading and release as a function of pH in water. These properties can determine the potential of these novel MNCs for biomedical applications. Therefore, the obtained data are expected to be useful for further development of novel formulations of EPI.

2. Results and discussion

Surface modification of the CoFe@Si nanoparticles with POM can affect EPI loading and release. The POMs used in this study are commercially available $H_3PW_{12}O_{40}$ (PW), $H_3PMo_{12}O_{40}$ (PMo), and $H_4SiW_{12}O_{40}$ (SiW). These POMs have numerous oxygen and protons in their structures and EPI has amino and OH functional groups (Figure 1). Therefore, hydrogen bonding could form between EPI and POMs. In addition, replacement of the surface protons of POMs with the positively charged EPI can lead to the formation of well-known ammonium salts of POMs[32,33] and induce ionic interactions between EPI and MNCs (Figure 1).

As ammonium salt formation progresses, exchange of the protons would change the acidity of the reaction medium. This pH change can be used to investigate the endpoint of the reaction in drug loading procedures. EPI loading on CoFe@Si and PW, SiW, and PMo functionalized CoFe@Si (designed as CoFe@Si-PW, CoFe@Si-SiW, and CoFe@Si-PMo, respectively) were studied. Figure 2 shows the profiles of drug loading on the surfaces of various CoFe@Si-POM MNCs. Drug loading contents, drug loading efficiencies, and acidities of MNCs are reported in the Table. EPI loading on CoFe@Si-POM MNCs were much higher than they were on CoFe@Si. Among the various MNCs, CoFe@Si-SiW showed the highest amount of EPI loading. Elemental analyses from ICP are also reported in the Table. All CoFe@Si-POM MNCs had relatively similar POM contents.

For efficient drug loading, it would be better to increase the loading efficiency. This increase in loading efficiency would decrease the loss of drugs. To reduce drug consumption, it is important to know how much drug will be loaded into the carrier. Herein, drug loading on MNCs was monitored simply using acid–base titration.

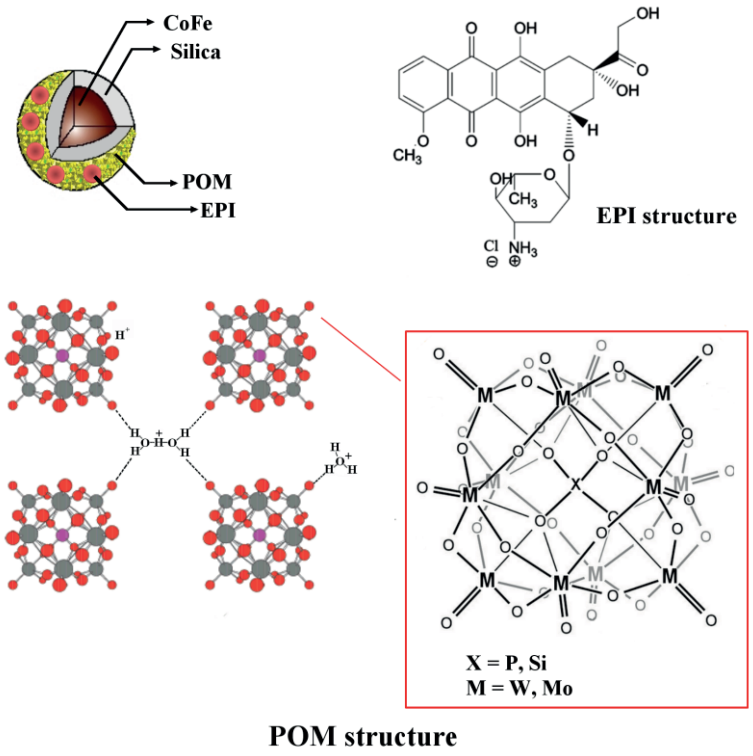

Figure 1. Schematic representation of EPI loaded POM-based MNCs, POM, and EPI structures.

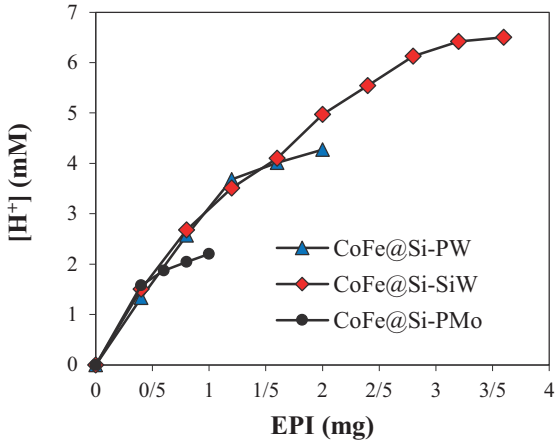

Figure 2. The EPI-loading profiles of various CoFe@Si-POM MNCs based on drug concentration and pH of the reaction medium.

Table. Characterization of EPI loaded MNCs.

Carrier	Drug loading content (wt.%)	Drug loading efficiency (%)	POM loading (wt.%)[a]
CoFe@Si	4.71	78.50	-
CoFe@Si-PW	18.09	90.45	18
CoFe@Si-SiW	35.23	97.86	15
CoFe@Si-PMo	7.16	71.60	13

[a] POM content in MNCs from ICP. Typically, the POM content from ICP was slightly lower than expected from the preparation stoichiometry.

This loading method is an improvement over the batch method in terms of simplicity and drug consumption, which was employed in our previous work.

The EPI release behavior was considered in PBS (pH = 7.4) and acetate buffer (pH = 5). The release profiles for various EPI-loaded MNCs are presented in Figure 3. In all cases, EPI release rate was increased in acidic medium (acetate buffer).

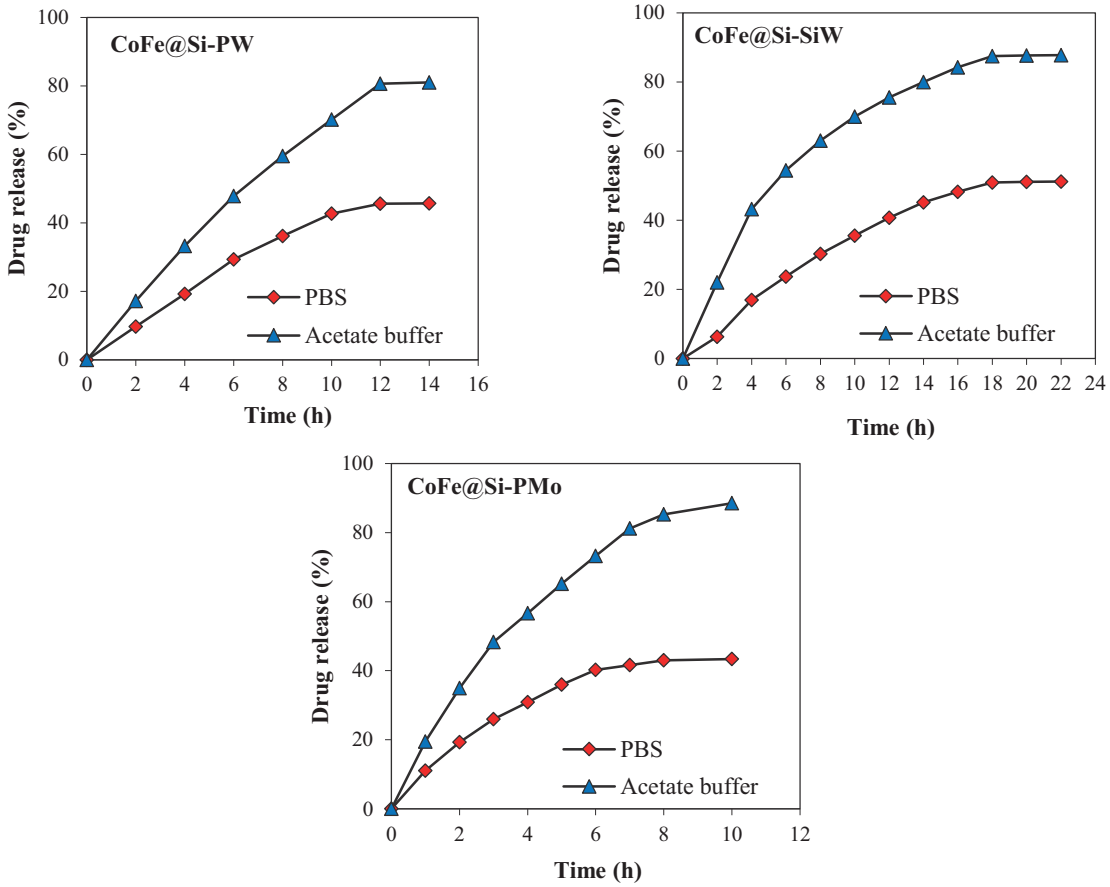

Figure 3. Release profiles of EPI from the EPI loaded CoFe@Si-POM MNCs in PBS (pH = 7.4) and acetate buffer (pH = 5).

All POM contents are strong acids and completely dissociated in aqueous solution. EPI is known as an amphiphilic weak base ($pK_a = 7.7$) due to its hydrophobic anthracycline and hydrophilic sugar moiety. As a weak base, the solubility of EPI is greatly influenced by the pH of the aqueous solution, e.g., a higher solubility in aqueous solution with a lower pH value.[34] Moreover, in acidic medium (acetate buffer), the protonation of an amino group leads to increased EPI release from the surface of MNCs.[32] Thus, POM-based MNCs may be used as a pH-sensitive carrier for EPI.

Based on the results above, CoFe@Si-SiW was selected as the best carrier in terms of drug loading content and drug loading efficiency. The morphological feature of the CoFe@Si-SiW MNC was investigated by scanning electron microscopy (SEM) and transmission electron microscopy (TEM). The TEM image (Figure 4) shows that CoFe@Si-SiW MNCs were spherical and have mean diameter of about 100 nm. Nevertheless, aggregates were observed in SEM and TEM images (Figures 4 and 5).

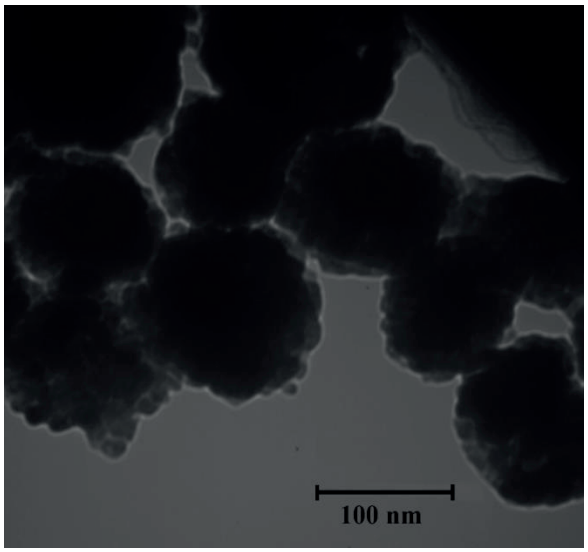

Figure 4. TEM image of CoFe@Si-SiW.

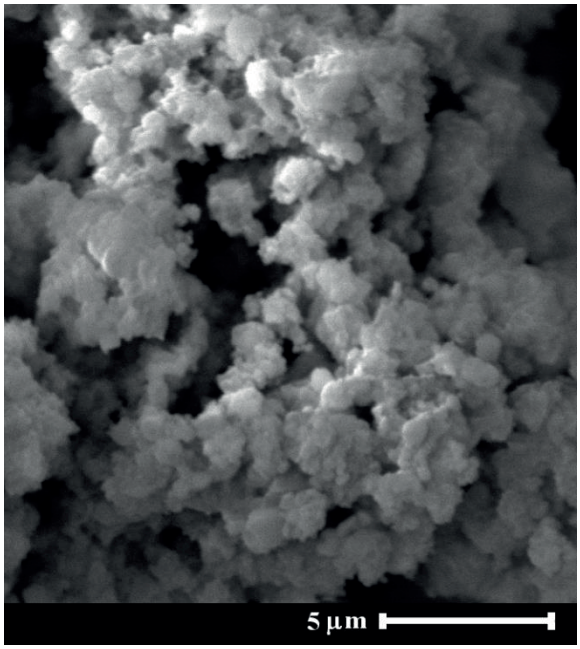

Figure 5. SEM image of CoFe@Si-SiW.

Figure 6 shows the studied wavelength dispersive X-ray (WDX) image. These images provide maps of individual elements of iron, cobalt, silica, and tungsten in cross section. A uniform distribution of SiW on the surface of CoFe@Si nanoparticles was observed.

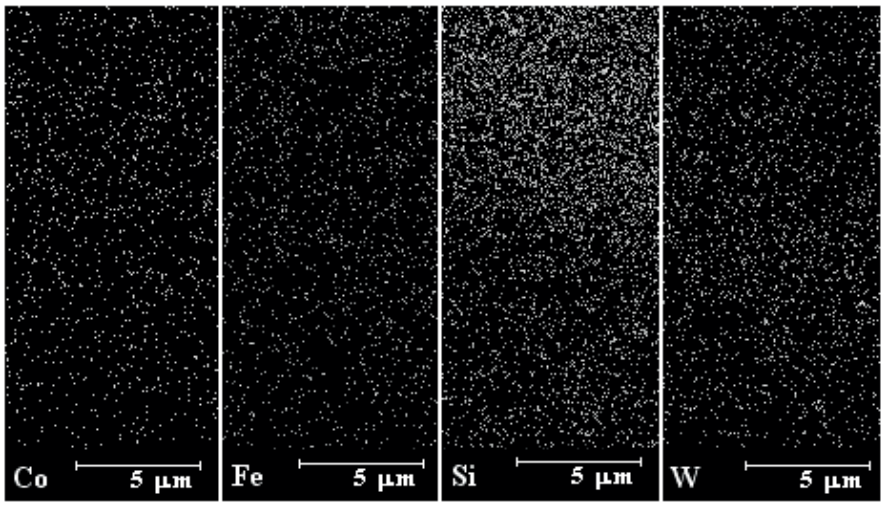

Figure 6. Elemental maps of Co, Fe, Si, and W atoms of CoFe@Si-SiW.

Fourier transform infrared (FTIR) spectra of CoFe@Si-SiW and EPI-loaded CoFe@Si-SiW are shown in Figures 7a and 7b. The bands at 981, 927, 882, and 786 cm^{-1} are attributed to W=O, Si–O, and W–O–W stretching modes of SiW.[35] The ammonium salt of SiW is characterized by a split in the W=O band (981 cm^{-1}). This doublet indicated a direct interaction between the polyanion and EPI cation.[35]

The size distributions for the CoFe@Si-SiW and EPI-loaded CoFe@Si-SiW were derived from a laser particle size analyzer and are illustrated in Figures 8a and 8b. Both of them exhibited monodisperse narrow

size distribution in water. CoFe@Si-SiW MNCs had a mean diameter of 157 nm with a polydispersity index of 0.48. EPI loaded CoFe@Si-SiW particles yielded a hydrodynamic diameter of 188 nm (polydispersity index of 0.39), which corresponds to a size increase of about 31 nm compared to EPI-free particles.

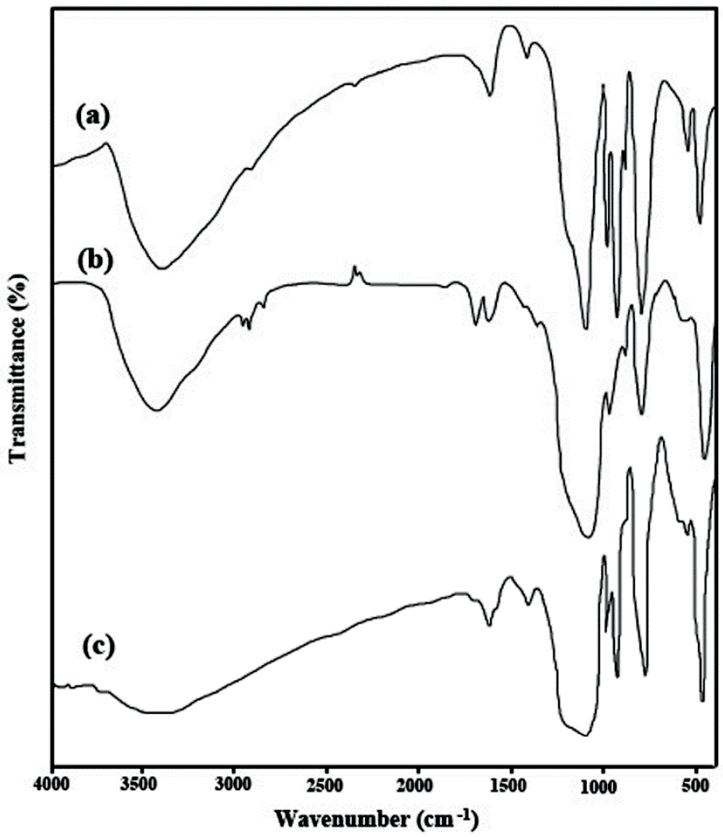

Figure 7. FTIR spectrum of (a) CoFe@Si-SiW, (b) EPI loaded CoFe@Si-SiW, and (c) CoFe@Si-SiW after release of EPI in acetate buffer.

It should be noted that the laser particle size analyzer determined the hydrodynamic diameter of the samples, whereas TEM represented the size in the dried samples. Clearly, hydrodynamic diameter was larger than the particle size obtained by TEM, due to the solvent effect.

Previously, only organic polymer was used as carrier for EPI delivery. This kind of carrier shows some disadvantages including limited chemical and mechanical stability, swelling, and susceptibility to microbiological attack. There is only one report of utilizing POM-based MNCs. In our previous work, the primary motivation was to create novel POM-based MNCs by PW modified silica encapsulated γ-Fe_2O_3. This carrier possesses high loading capacity for epirubicin (20.6 wt.%) and high drug loading efficiency (82.6%). However, the effects of the type of POM and the change in pH during the loading process have remained a challenge. In the present work, both of these parameters were investigated. Drug loading was monitored simply using acid–base titration, which is an improvement over the batch method in terms of simplicity and drug consumption. Based on these investigations, an efficient EPI-delivery system was introduced. CoFe@Si-SiW particles, as the best MNC, showed high EPI-loading capability (35.2 wt.%) with excellent EPI-loading efficiency (97.9%) compared to previous work. EPI release was faster in acetate buffer (87.7%) compared to PBS (51.2%). As a result, this

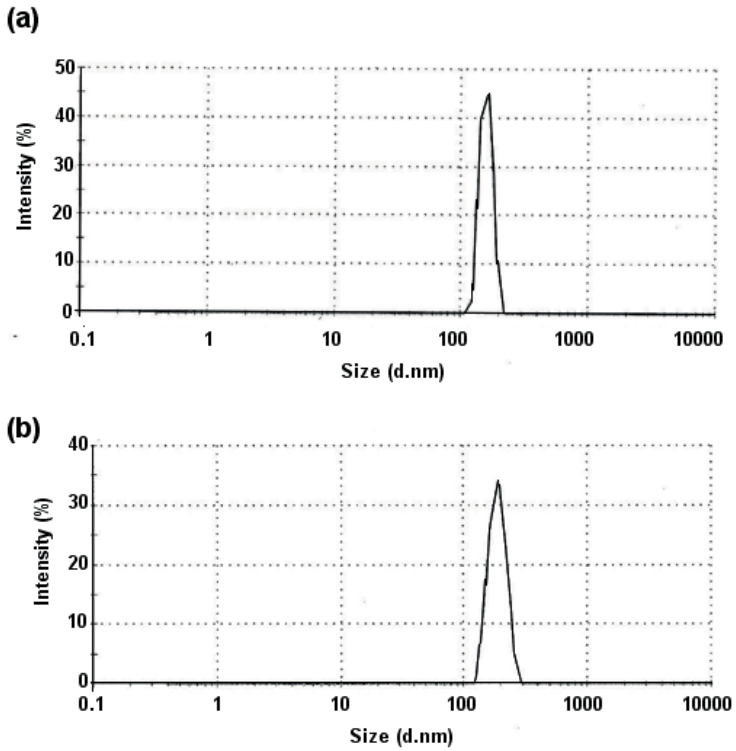

Figure 8. Particle size distribution of (a) CoFe@Si-SiW and (b) EPI loaded CoFe@Si-SiW.

pH-sensitive system can moderate the cytotoxicity of EPI. Moreover, these MNCs may be used in MRI as a contrast agent. It is expected that these data will be useful for further development of novel MNCs of EPI and similar anthracyclines.

3. Experimental

3.1. General

$H_3PW_{12}O_{40}$ (PW), $H_3PMo_{12}O_{40}$ (PMo), and $H_4SiW_{12}O_{40}$ (SiW) were purchased from Aldrich. EPI was obtained from Shandong New Time Pharmaceutical Co., Ltd., China. All chemicals were analytical grade. All solutions were prepared using distilled water.

The SEM image was obtained using Philips XL 30 and S-4160 with gold coating. The TEM image was obtained using a TEM microscope (Philips CM 120 KV, the Netherlands). A laser particle size analyzer (HPPS 5001, Malvern, UK) was used to determine the particle size distribution. The POM content in the MNC was measured using inductively coupled plasma atomic emission spectroscopy (ICP-AES) on a Spectro Ciros CCD spectrometer. UV-vis absorption spectra were obtained using an Agilent (8453) UV-vis diode-array spectrometer. FTIR spectra were recorded with KBr pellets using a FTIR spectrometer (ALPHA).

3.2. Preparation of POM functionalized CoFe@Si

Cobalt ferrite nanoparticles were prepared by co-precipitation method. An aqueous mixture of $CoCl_2.6H_2O$ (25 mL, 0.1 M) and $FeCl_3.6H_2O$ (25 mL, 0.2 M) was prepared and the solution was kept at 70 °C. Then

sodium hydroxide solution (24 mL, 3.0 M) was added. The dark brown precipitate obtained was washed with distilled water several times to achieve a brown magnetic dispersion that has high stability.

CoFe@Si nanoparticles were obtained using the Stöber process.[36] Then the MNCs were functionalized with PW, PMo, and SiW using the impregnation method. Typically, 1.0 g of CoFe@Si was impregnated with methanol solution of PW (0.25 g in 5 mL) and stirred at about 70 °C for 72 h. The prepared samples were collected using a magnet and dried in a vacuum overnight.

3.3. EPI-MNCs preparation

For the preparation of EPI-loaded MNCs, 10 mg of CoFe@Si-POM was suspended in 2 mL of phosphate buffered saline (PBS) (pH = 7.4) with magnetic stirring at 37 °C. An aqueous solution of EPI (2 mg/mL) was added dropwise to the CoFe@Si-POM suspension. The pH changes in CoFe@Si-POM suspension were measured during the addition of EPI solution using a Hanna 302 pH meter. When the pH was relatively stable, the EPI-loaded MNCs were separated using a magnet and the supernatant was used for the measurements of loading efficiency and drug loading content. The free EPI content in the supernatant was quantified using UV-vis spectroscopy. The absorbance of the solution was measured at 480 nm for EPI. The loading efficiency and drug loading content were calculated using the following equations:

$$\text{Loading efficiency} = \frac{\text{W total drug W drug in supernatant}}{\text{W total drug}} \times 100$$

$$\text{Drug loading content} = \frac{\text{W total drug W drug in supernatant}}{\text{W carrier}} \times 10$$

3.4. EPI release

EPI release was investigated at 37 °C in PBS (pH = 7.4) and acetate buffer (pH = 5). EPI-loaded MNCs were dispersed in 5 mL of each buffer with magnetic stirring. The supernatant was withdrawn at predetermined time intervals and analyzed by UV-vis spectroscopy. At the same time, 5 mL of fresh buffer was added for the next experiments. Stability of the carrier was checked after releasing of the drug in acetate buffer. The structure of the carrier does not change with changing pH according to FTIR (Figure 7c).

Acknowledgments

The authors thank the Razi University Research Council for its support of this work.

References

1. Gultepe, E.; Nagesha, D.; Sridhar, S.; Amiji, M. *Adv. Drug. Deliv. Rev.* **2010**, *62*, 305–315.
2. He, Y.; Fan, C.; Lee, S. T. *Nano Today* **2010**, *5*, 282–295.
3. Lee, H.; Mi, K. Y.; Park, S.; Moon, S.; Jung, J. M.; Yong, Y. J.; Kang, H. W.; Jon, S. *J. Am. Chem. Soc.* **2007**, *129*, 12739–12745.
4. Wang, A. Z.; Bagalkot, V.; Vasilliou, C. C.; Gu, F.; Alexis, F.; Zhang, L.; Shaikh, M.; Yuet, K.; Cima, M. J.; Langer, R.; et al. *Chem. Med. Chem.* **2008**, *3*, 1311–1315.
5. Weissleder, R. *Science* **2006**, *312*, 1168–1171.
6. Arruebo, M.; Pacheco, R. F.; Ibarra, M. R.; Santamaría, J. *Nano Today* **2007**, *2*, 22–32.

7. Kale, S. N.; Jadhav, A. D.; Verma, S.; Koppikar, S. J.; Kaul-Ghanekar, R.; Dhole, S. D.; Ogale, S. B. *Nanomedicine* **2012**, *8*, 452–459.
8. Jabir, N. R.; Tabrez, S.; Ashraf, G. M.; Shakil, S.; Damanhouri, G. A.; Kamal, M. A. *Int. J. Nanomedicine* **2012**, *7*, 4391–4408.
9. Goodwin, S.; Peterson, C.; Hob, C.; Bittner, C. *J. Magn. Magn. Mater.* **1999**, *194*, 132–139.
10. Knežević, N. Z.; Slowing, I. I.; Lin, V. S. Y. *Chem. Plus. Chem.* **2012**, *1*, 48–55.
11. Steinfeld, U.; Pauli, C.; Kaltz, N.; Bergemann, C.; Lee, H. T. *Int. J. Pharm.* **2006**, *311*, 229–236.
12. Arruebo, M.; Fernández-Pacheco, R.; Irusta, S.; Arbiol, J.; Ibarra, M. R.; Santamaria, J. *Nanotechnology* **2006**, *17*, 4057–4064.
13. Ma, Y.; Manolache, S.; Denes, F.; Vail, D.; Thamm, D.; Kurzman, I. *J. Mater. Eng. Perform.* **2006**, *15*, 376–382.
14. Ma, Y.; Manolache, S.; Denes, F.; Thamm, D.; Kurzman, I.; Vail, D. *Biomater. J. Sci. Polym. Ed.* **2004**, *15*, 1033–1049.
15. Etrych, T.; Jelínková, M.; Říhová, B.; Ulbrich, K. *J. Control. Release* **2001**, *73*, 89–102.
16. Leakakos, T.; Ji, C.; Lawson, G.; Peterson, C.; Goodwin, S. *Cancer Chemother. Pharmacol.* **2003**, *51*, 445–450.
17. Rudge, S.; Peterson, C.; Vessely, C.; Koda, J.; Stevens, S.; Catterall, L. *J. Control. Release* **2001**, *74*, 335–340.
18. Chen, J.; Guo, Z.; Wang, H. B.; Gong, M.; Kong, X. K.; Chen, Q. W.; Xia, P. *Biomaterials* **2013**, *34*, 571–581.
19. Oliveira, H.; Andrés, E. P.; Thevenot, J.; Sandre, O.; Berra, E.; Lecommandoux, S. *J. Control. Release* **2013**, *169*, 165–170.
20. Jalalian, S. H.; Taghdisi, S. M.; Kalat, S. A. M.; Jaafari, M. R.; Abnous, K.; Lavaee, P.; Naghibi, S.; Hamedani, N. S.; ZandKarimi, M.; Danesh, N. M.; et al. *Eur. J. Pharm. Sci.* **2013**, *50*, 191–197.
21. Minotti, G.; Menna, P.; Salvatorelli, E.; Cairo, G.; Gianni, L. *Pharmacol. Rev.* **2004**, *56*, 185–229.
22. Gianni, L.; Norton, L.; Wolmark, N.; Suter, T. M.; Bonadonna, G.; Hortobagyi, G. N. *J. Clin. Oncol.* **2009**, *27*, 4798–4808.
23. Cersosimo, R. J.; Hong, W. K. *J. Clin. Oncol.* **1986**, *14*, 425–439.
24. Bonadonna, G.; Gianni, L.; Santoro, A.; Bonfante, V.; Bidoli, P.; Casali, P.; Demicheli, R.; Valagussa, P. *Ann. Oncol.* **1993**, *4*, 359–369.
25. Lübbe, A. S.; Alexiou, C.; Bergemann, C. *J. Surg. Res.* **2001**, *95*, 200–206.
26. Wang, S. *Micropor. Mesopor. Mater.* **2009**, *117*, 1–9.
27. Geisberger, G.; Paulus, S.; Gyenge, E. B.; Maake, C.; Patzke, G. R. *Small* **2011**, *7*, 2808–2814.
28. Guo, R.; Cheng, Y.; Ding, D.; Li, X.; Zhang, L.; Jiang, X.; Liu, B. *Macromol. Biosci.* **2011**, *11*, 839–847.
29. Rhule, J. T.; Hill, C.L.; Judd, D. A. *Chem. Rev.* **1998**, *98*, 327–358.
30. Yanagie, H.; Ogata, A.; Mitsui, S.; Hisa, T.; Yamase, T.; Eriguchi, M. *Biomed. Pharmacother.* **2006**, *60*, 349–352.
31. Zhai, F.; Li, D.; Zhang, C.; Wang, X.; Li, R. *Eur. J. Med. Chem.* **2008**, *43*, 1911–1917.
32. Van, J.; Smit, R.; Jacobs, J. J.; Robb, W. *J. Inorg. Nucl. Chem.* **1959**, *12*, 95–103.
33. Katsoulis, D. E. *Chem. Rev.* **1998**, *98*, 359–387.
34. Maurer-Spurej, E.; Wong, K. F.; Maurer, N.; Fenske, D. B.; Cullis, P. R. *Biochim. Biophys. Acta* **1999**, *1416*, 1–10.
35. Pope, M. T. *Heteropoly and Isopoly Oxometalates*; Springer-Verlag: Berlin, Germany, 1983.
36. Stöber, W.; Fink, A.; Bohn, E. *J. Colloid. Interface. Sci.* **1968**, *26*, 62–69.